



Study of two approaches for the process water management from hydrothermal carbonization of swine manure: Anaerobic treatment and nutrient recovery

R.P. Ipiales^{a,b}, G. Lelli^a, E. Diaz^a, E. Diaz-Portuondo^b, A.F. Mohedano^a, M.A. de la Rubia^{a,*}

^a Chemical Engineering Department, Universidad Autonoma de Madrid, 28049, Madrid, Spain

^b Arquimea Agrotech, 28400, Collado Villalba, Madrid, Spain

ARTICLE INFO

Keywords:

Anaerobic digestion
High-rate anaerobic reactor
Hydrothermal carbonization
Phosphorus recovery
Process water

ABSTRACT

Hydrothermal carbonization (HTC) is a promising alternative to transform biomass waste into a solid carbonaceous material (hydrochar) and a process water with potential for material and energy recovery. In this study, two alternatives for process water treatment by conventional and acid-assisted HTC of swine manure are discussed. Process water from conventional HTC at 180 °C showed high biodegradability (55% COD removal) and methane production ($\sim 290 \text{ mL STP CH}_4 \text{ g}^{-1} \text{ COD}_{\text{added}}$) and the treatment in an upflow anaerobic sludge blanket reactor allowed obtaining a high methane production yield ($1.3 \text{ L CH}_4 \text{ L}^{-1} \text{ d}^{-1}$) and COD removal ($\sim 70\%$). The analysis of the microbiota showed a high concentration of Synergistota and Firmicutes phyla, with high degradation of organic nitrogen-containing organic compounds. Acid-assisted HTC proved to be a viable option for nutrient recovery (migration of 83% of the P to the process water), which allowed obtaining a solid salt by chemical precipitation with $\text{Mg}(\text{OH})_2$ (NPK of 4/4/0.4) and MgCl_2 (NPK 8/17/0.5), with a negligible content of heavy metals. The characteristics of the precipitated solid complied with the requirements of European Regulation (2019)/1009 for fertilizers and amendments in agricultural soils, being a suitable alternative for the recycling of nutrients from wastes.

1. Introduction

The swine industry is one of the most significant agro-industries in the European Union (EU), with an estimated of 142 million heads in 2020 and represent the largest livestock category in the EU, followed by bovines (around 87 million heads) (EUROSTAT, 2020). This industry plays a concerning role in contributing to as much as 11% (6 million tons of CO_2e) of the total greenhouse gas (CH_4 , NH_3 , N_2O and CO_2) ascribe of this sector, with up to 75% of these emissions stemming from the management of swine manure (SM) (EUROSTAT, 2020; Köninger et al., 2021). This livestock waste is traditionally intended for composting due to high organic matter and nutrients which can be returned back to the soils (He et al., 2023), although beneficial for agricultural soils, emits CH_4 , CO_2 , NH_3 , and N_2O , lead to nutrient runoff P and N as well is not effectively remove harmful components like heavy metals, pharmaceuticals, or microorganisms (Bianchini et al., 2016; Bloem et al., 2017). Anaerobic digestion (AD) is another common practice to transform SM into a biogas rich in methane ($\sim 70\% \text{ CH}_4$ and $30\% \text{ CO}_2$) and remove

organic matter (Zahedi et al., 2022). Anaerobic digestion of SM streams is a complex challenge, due to the high COD and $\text{NH}_3\text{-N}$ concentrations low C/N ratio as well inhibitory components such as emergent contaminants or heavy metals (Bloem et al., 2017).

Hydrothermal carbonization (HTC) is a thermochemical technology that offers a promising alternative for waste management with high moisture content ($>40\%$) (Heidari et al., 2020). HTC is carried out at mild temperatures (180–250 °C), low resident time (5–240 min) and autogenous pressure, which involves a series of complex chemical reactions, including hydrolysis, dehydration, decarboxylation, and aromatization, that transform the organic compounds present in the biomass into a stable, sanitized, and homogeneous product (hydrochar), and a liquid fraction (process water) with a high energy and material potential valorization (Becker et al., 2019). Hydrochar is a versatile material for use as biofuel, soil amendment, carbon storage or carbon active precursor (Khosravi et al., 2022; Sharma et al., 2020). The process water, which requires further treatment, contains a high concentration of organic matter and nutrients, which allows its possible utilization. AD

* Corresponding author.

E-mail address: angeles.delarubia@uam.es (M.A. de la Rubia).

<https://doi.org/10.1016/j.envres.2024.118098>

Received 30 October 2023; Received in revised form 29 December 2023; Accepted 2 January 2024

Available online 5 January 2024

0013-9351/© 2024 The Author(s). Published by Elsevier Inc. This is an open access article under the CC BY-NC license (<http://creativecommons.org/licenses/by-nc/4.0/>).

Table 1
Main characteristics of swine manure^a.

		Mineral species (g kg ⁻¹)		Heavy metals (mg kg ⁻¹)	
pH	7.9 (0.1)	Al	1.0 (0.2)	Cd	0.4 (0.1)
TS (g L ⁻¹)	57.9 (0.8)	Ca	34.3 (2.5)	Co	1.3 (0.1)
VS (g L ⁻¹)	41.2 (0.4)	Fe	1.4 (0.1)	Cr	10.5 (0.2)
TCOD (g L ⁻¹)	67.2 (1.1)	K	32.7 (1.4)	Cu	121.2 (1.2)
TOC (g L ⁻¹)	3.7 (0.1)	Mg	13.0 (1.2)	Ni	4.0 (0.1)
TVFA (g acetic acid L ⁻¹)	1.0 (0.1)	Na	10.0 (0.1)	Pb	3.5 (0.1)
TKN (g L ⁻¹)	3.9 (0.2)	P	30.3 (1.5)	Zn	1110.5 (1.5)
TAN (g L ⁻¹)	2.9 (0.1)				
NO ₃ -N (mg L ⁻¹)	11.2 (0.0)				
NO ₂ -N (mg L ⁻¹)	1.7 (0.1)				

^a Average values of three determinations with standard deviations in brackets.

stands out as one of the most attractive complementary processes for process water valorization from HTC.

Most studies on anaerobic treatment of HTC process water focus predominantly on assessing biochemical methane potential. Studies on continuous anaerobic treatment of process water showed high methane production performance (135–240 mL CH₄ g⁻¹ COD_{removed}) and organic matter removal of 40–70%, comparable to batch trials (Ahmed et al., 2021; Wirth and Mumme, 2013). Various configurations of continuous anaerobic digesters, such as anaerobic filters, continuous stirred tank reactors, and upflow anaerobic sludge blanket (UASB) reactors have been used, along with different operational conditions, such as hydraulic retention time (HRT: 3–5 days) and organic loading rate (OLR: 1–15 g COD L⁻¹·d⁻¹) (Liu et al., 2021; Weide et al., 2019a; Wirth and Mumme, 2013).

Another emerging alternative for the process water utilization is the recovery of solubilized nutrients from feedstock as phosphorus-rich salts that can be applied on agricultural soils as inorganic fertilizers (Becker et al., 2019; Sarrion et al., 2023). Previous studies have shown the potential to recover nutrients from process water, achieving up to 99% of P as PO₄-P, 60% of N as NH₃-N, and other essential macronutrients such as Ca, Mg, K (Ipiales et al., 2023a; Numviyimana et al., 2022). According to these studies, the content of heavy metals in the precipitated solids was below the limit established in the European Union Regulation 2019/1009 (European Union, 2019) for the use in agricultural soils.

The work analyzes and compares two possible ways for valorizing process water, through methane production by anaerobic digestion and nutrient recovery. The research delves into the composition and diversity of organic compounds in the process water under different operating conditions (temperature and time). The anaerobic biodegradability of the process water is evaluated in batch experiments for subsequent continuous scale-up for methane production and organic matter removal performance. In addition, the inoculum composition and its adaptability to a complex substrate such as process water is also studied. Nutrient recovery is analyzed using two magnesium salts for the formation of P-rich species, as well as the mineral composition of the precipitated salts.

2. Materials and methods

2.1. Feedstock

Swine manure was collected from a swine farm located in Avila (Spain) and stored at -20 °C until used. Table 1 shows the main characteristics of SM.

2.2. HTC experiments

HTC experiments were carried out in an electrically heated Zipper-Clave® pressure vessel (4 L). Swine manure (1.5 kg) was treated in each run, three different temperatures were tested (180 °C, 210 °C, and

230 °C) in triplicate. The target temperature was reached with a heating rate of 3 °C min⁻¹ and maintained for 1 h. Acid-assisted HTC experiments were performed at the same temperatures and reaction time as conventional HTC but adding 0.5 M HCl. The reactions were stopped by an internal coil through which tap water with a cooling ramp 10 °C min⁻¹. The slurry (hydrochar and process water) was separated by centrifugation (Orto Alresa centrifuge at 8000 rpm for 10 min) and vacuum filtration (0.45 µm). The process water was stored at 4 °C for subsequent nutrient recovery and batch and continuous AD runs. Process water (PW) and acid process water (APW) were labelled according to the carbonization temperature i.e., PW180, PW210, and PW230 for conventional HTC, and APW180, APW210, and APW230 for acid-assisted HTC, respectively.

2.3. Nutrients recovery

A sample of 250 mL of the process water obtained at 180 °C (PW180 and APW180) were used to phosphorus chemical precipitation. Two magnesium salts, MgCl₂ (Panreac) and Mg(OH)₂ (Panreac), were used to promote the formation of P-rich species by in the stoichiometric ratio 1:1.3:1 M of NH₄:Mg:PO₄ according to Weideler et al. (2008). A solution of 2 M NaOH was added to both process waters to increase the pH to 9 while mixing for 20 min at 300 rpm. The precipitated solid was separated by filtration through 0.45 µm and oven dried at 105 °C overnight.

2.4. Anaerobic digestion

Granular anaerobic sludge from an industrial digester processing brewery wastewater was used as inoculum for batch and continuous experiments. The inoculum characteristics were as follow: TS 45.6 (1.1) g L⁻¹, volatile solids (VS) 38.3 (0.9) g L⁻¹ and total chemical oxygen demand (TCOD) 65.9 (1.6) g O₂ L⁻¹.

2.4.1. Anaerobic digestion in batch experiments

Batch runs were performed in 120 mL glass serum flasks, with an inoculum concentration of 15 g VS L⁻¹ and an inoculum-to-substrate ratio (ISR) of 2 on a VS basis. The time course was followed by using ten vials for each of the process water samples obtained at the three HTC temperatures (PW180, PW210, PW230), the process water from acid-assisted HTC at 180 °C (APW180) as well as raw SM tested. Basal medium with macro (NH₄Cl, 280 mg L⁻¹; K₂HPO₄, 250 mg L⁻¹; MgSO₄·7H₂O, 100 mg L⁻¹; CaCl₂·2H₂O, 10 mg L⁻¹; yeast extract, 100 mg L⁻¹) and micronutrients (FeCl₂·4H₂O, 2 mg L⁻¹; CoCl₂·6H₂O, 2 mg L⁻¹; MnCl₂·4H₂O, 0.5 mg L⁻¹; AlCl₃·6H₂O, 0.09 mg L⁻¹; (NH₄)₆Mo₇O₂₄·4H₂O, 0.05 mg L⁻¹; H₃BO₃, 0.05 mg L⁻¹; ZnCl₂, 0.05 mg L⁻¹; CuCl₂·2H₂O, 0.038 mg L⁻¹) was prepared and dosed as described by Angelidaki and Sanders (2004), after that each vial was filled up to 60 mL with deionized water. The vials were sealed with rubber stoppers and metallic crimps and then were purged with N₂ for 3 min to ensure anaerobic conditions. Finally, the vials were held in a thermostatic shaking water bath at 120 rpm equivalent stirring and mesophilic temperature 35 °C. Seven of them were sacrificed: two during the first three days and then every week. The remaining three vials were used for tracking the methane production. Moreover, triplicate blank samples with no substrate were run to determine the background methane from the inoculum and three starch positive controls using soluble potato starch (Panreac), that yielded 351 (10) mL STP CH₄ g⁻¹ COD_{added}.

2.4.2. Anaerobic digestion in continuous experiments

Considering the results obtained in the batch tests, PW180 was used as substrate for AD using an UASB reactor of 5.4 L net volume, made of polymethyl methacrylate (Fig. S1). The reactor was inoculated with 1.6 kg of granular sludge (a height of 20 cm of inoculum) and started by feeding glucose (G) at an OLR of 5 g COD L⁻¹·d⁻¹ and operating at 1 d of

Table 2
UASB reactor feed composition.

Phase	Time (d)	PW/G (on a COD basis)
Startup	1–17	0/100
I	18–33	10/90
II	34–60	20/80
III	61–87	30/70
IV	88–100	40/60
V	101–117	50/50
VI	118–124	60/40
VII	125–145	75/25

HRT. Glucose was gradually replaced by PW180 (see Table 2). The experiment was carried out at mesophilic temperature 35 (1) °C, which was kept by an external jacket filled with hot water circulating in a water bath. Further, a pH buffer (NaHCO₃ as 1 g L⁻¹) and a solution containing macro and micronutrients (1 mL L⁻¹) (Villamil et al., 2018) were added to the feeding mixture. Biogas collected from the gas-solid-liquid separator on top of the reactor was directed to a gas counter (MilliGascounter with a 3.16 mL drum volume, Ritter) to measure the daily biogas production and then collected into a 10 L gas bag (multi-layer foil gas samplings bags, Supelco) for further analysis.

2.5. Analytical methods

Swine manure, process water as well as effluents from nutrient recovery stage and AD in batch and continuous assays were characterized by pH (Crison 20 Basic pH-metre). The TS and VS were measured according to standard methods 2540B and 2540E, respectively (APHA, 2005). TCOD was determined according to Raposo et al. (2008). Soluble COD (SCOD) was determined using APHA 5220D method (APHA, 2005). Total organic carbon (TOC) was determined by a Shimadzu TOC-VCPN (Shimadzu; Kyoto, Japan) analyzer while, VFA was determined by gas chromatography (GC) on a Varian 430-GC instrument (Varian 430-GC; Markham, Canada) equipped with a flame ionization detector (FID) and a capillary column packed with Nukol (nitroterephthalic acid-modified polyethylene glycol; (De la Rubia et al., 2018)). The total Kjeldahl nitrogen (TKN) and total ammonia nitrogen (TAN) were determined by methods 4500D and 4500E, respectively, (APHA, 2005). Organic nitrogen (Org-N) was determined by the difference between TKN and TAN. Total alkalinity (TA) was measured by 2320B method (APHA, 2005). NO₃-N, NO₂-N and PO₄-P were measured photometri-

Table 3
Main characteristics of process water* from conventional and acid-assisted HTC at several temperatures.

	PW180	PW210	PW230	APW180	APW210	APW230
pH	8.6 (0.3) ^a	9.3 (0.3) ^a	9.2 (0.3) ^a	2.8 (0.4) ^a	2.6 (0.2) ^a	2.9 (0.3) ^a
TS (g L ⁻¹)	24.0 (1.2) ^a	21.7 (0.8) ^a	18.9 (1.6) ^b	38.4 (1.1) ^c	37.7 (0.3) ^c	37.0 (1.2) ^c
VS (g L ⁻¹)	18.3 (0.5) ^a	15.0 (0.7) ^b	12.1 (0.2) ^c	24.7 (0.4) ^d	25.6 (0.7) ^d	24.5 (1.3) ^d
TCOD (g L ⁻¹)	30.5 (1.2) ^a	27.3 (0.2) ^b	27.8 (0.6) ^b	28.4 (0.9) ^b	33.3 (0.8) ^c	33.8 (0.6) ^c
TOC (g L ⁻¹)	9.6 (0.3) ^a	9.2 (0.4) ^a	9.1 (0.3) ^a	9.0 (0.3) ^a	8.8 (0.2) ^a	8.3 (0.2) ^b
TVFA (g acetic acid L ⁻¹)	1.8 (0.1) ^a	2.0 (0.1) ^a	1.9 (0.1) ^a	1.7 (0.3) ^a	1.8 (0.1) ^a	1.7 (0.1) ^a
TKN (g L ⁻¹)	1.7 (0.1) ^a	2.1 (0.2) ^b	1.9 (0.2) ^a	3.5 (0.4) ^c	3.8 (0.3) ^c	3.7 (0.3) ^c
TAN (g L ⁻¹)	1.1 (0.1) ^a	1.6 (0.2) ^b	1.4 (0.2) ^{a,b}	3.4 (0.2) ^c	3.7 (0.3) ^c	3.7 (0.2) ^c
NO ₃ -N (mg L ⁻¹)	11.7 (0.1) ^a	12.0 (0.2) ^a	12.9 (0.0) ^b	11.3 (0.0) ^a	11.7 (0.0) ^a	10.1 (0.0) ^c
NO ₂ -N (mg L ⁻¹)	3.5 (0.2) ^a	2.7 (0.2) ^a	2.2 (0.1) ^b	0.6 (0.0) ^c	0.8 (0.0) ^c	1.2 (0.0) ^d
PO ₄ -P (mg L ⁻¹)	55.6 (2.1) ^a	62.7 (1.1) ^a	70.6 (0.7) ^b	416.5 (0.7) ^c	374.7 (2.1) ^d	371.9 (4.2) ^d

*Average values of three determinations with standard deviations are shown in brackets.

a,b,c,d Means with different superscript significant differ (p < 0.05).

patterns were recorded at a scanning speed of 0.05°/2θ ranging from 5° to 80°.

Biogas composition (H₂, CO₂, CH₄ and H₂S) was measured in a GC-Thermo Scientific Trace 1300 (Thermo Scientific; Villebon, France) equipped with a thermal conductivity detector (TCD) and a 8 ft × 1/8 in SS column packed with HayeSep Q 80/100 mesh (De la Rubia et al., 2018).

COD balance was performed using the Eqs. (1) and (2) as follows:

$$COD_{IN} = COD_{OUT} + COD_{CH_4} + COD_{CO_2} + COD_A \quad (1)$$

$$COD_{IN} \times V_{IN} = COD_{OUT} \times V_{OUT} + \frac{COD_{consumed}}{L_{Biogas}} \times \left(\frac{L_{Biogas}}{L_{CH_4}} \right) \times V_{CH_4} + \frac{COD_{consumed}}{L_{Biogas}} \times \left(\frac{L_{Biogas}}{L_{CO_2}} \right) \times V_{CO_2} + COD_A \quad (2)$$

cally using a Hach Lange Spectrophotometer (DR3900; Düsseldorf, Germany) using LCK 340 (NO₃-N), LCK 342 (NO₂-N) and LCK350 (PO₄-P) cuvette tests. The conductivity of process water were measured with a conductivity meter Mettler Toledo S400. Chemical species from process water were identified by gas chromatography/ion-trap mass spectrometry (GC-MS) on a CP-3800/Saturn 2200 instrument equipped with a Varian CP-8200 autosampler injector and a Carbowax/Divinyl benzene Yellow Green solid-phase micro-extractor, and fitted with a Factor Four VF-5 MS capillary column (De la Rubia et al., 2018).

The mineral and heavy metal content of the SM and the precipitated solids from the nutrient recovery stage were quantified by inductively coupled plasma atomic emission spectroscopy (ICP-OES) on an Elan 6000 Sciex instrument (PerkinElmer; Santa Clara, United States). Crystal structure of the solid precipitated from the nutrient recovery stage was performed by X-ray diffraction (XRD; Hertogenbosch, Netherlands), using a Siemens D5000 diffractometer employing Cu-Kα radiation. The

where COD_{IN}, COD_{OUT}, represent the concentrations of COD expressed in g COD L⁻¹, and V_{IN}, and V_{OUT} the volumes measured in L, of the feed and effluent, respectively. V_{Biogas} is the volume of biogas quantified using the MilliGascounter. The L_{Biogas} L_{CH₄,CO₂}⁻¹ ratio is the percentage of CH₄ or CO₂ within the biogas, assessed through GC analysis. Additionally, COD_A, as defined by elsewhere (Buckel, 2021; Oelgeschläger and Rother, 2008), stands for the chemical oxygen demand necessary for microorganism metabolism. It is determined by computing the variance between COD_{IN}, COD_{OUT}, COD_{CH₄}, and COD_{CO₂}.

2.6. Microbial and granulometric biomass analysis

Granular sludge samples from the bottom of the UASB reactor were collected during the stationary phase in the start-up phase, stages III and VII, days 15, 85 and 140, respectively (see Table 2), to reveal the effects of OLRs on microbial community. Each sludge sample was mixed

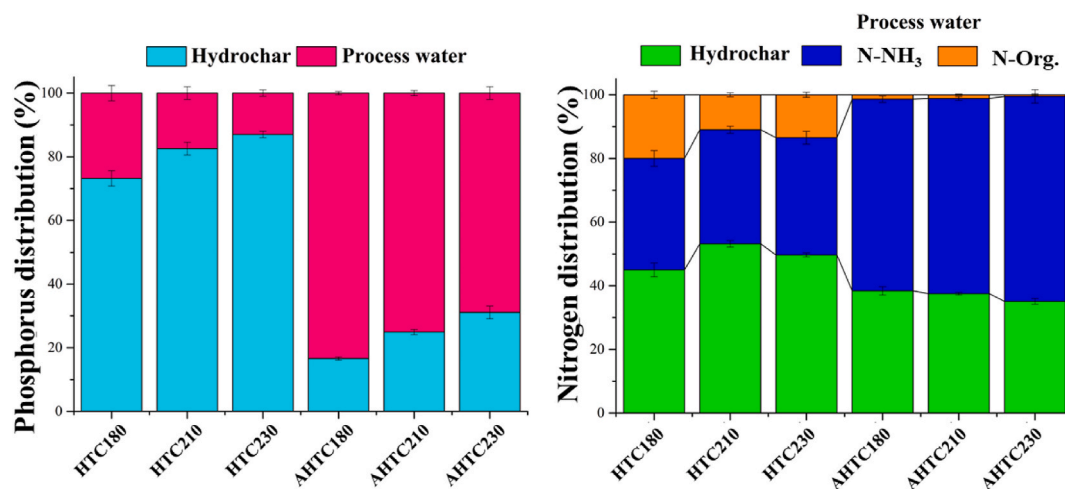


Fig. 1. Phosphorus and nitrogen distribution into hydrochar and process water from conventional and acid-assisted HTC.

thoroughly before collection and then stored at -20°C . These samples were conducted for high throughput 16S rRNA gene sequencing analysis. The primers of 341F (5'-CCTACGGGNGGCWGCAG-3') and 805R (5'-GACTACHVGGGTATCTAATCC-3') were used for amplification of the V3–V4 region of bacterial 16S rRNA gene. After 16S rDNA gene amplification, both the multiplexing step and size verification were performed, using Nextera XT Index Kit (FC-131-1096) and Bioanalyzer DNA 1000 chip, respectively. Libraries were sequenced using a $2 \times 300\text{bp}$ paired-end run (MiSeq Reagent kit v3 (MS-102-3001)) on a MiSeq Sequencer according to manufacturer's instructions (Illumina).

2.7. Statistical analysis

Statistical analysis of the results was performed by analysis of variance (ANOVA) using Origin 8.1 software. Fisher's least significant difference (Fisher's LSD) was calculated at a confidence level of $p < 0.05$. To identify significant differences, multiple comparisons were performed.

3. Results and discussion

3.1. Process water characterization

Table 3 shows the main characteristics of process water obtained in conventional and acid-assisted HTC. The addition of acid to the reaction significantly influenced ($p > 0.05$) on the content of TS and VS, as well $\text{PO}_4\text{-P}$, nitrogen (TKN and TAN) and conductivity, but showed a minor impact ($p < 0.05$) on organic matter content (TCOD, TOC and TVFA). As expected, the addition of acid decreased the pH (~ 3), while the conventional HTC process water presented a basic pH (~ 9). A high pH value (> 8) in HTC process water is common for wastes with high ammonia nitrogen, alkaline components and carbonates, especially from those with a low C/N ratio, such as sewage sludge or animal manure. In contrast, for process water from wastes with high C content (carbohydrates or lignocellulosic components), acidic pH values (even lower than 5) have been observed due to the formation of short-chain organic acids, particularly acetic acid (Funke and Ziegler, 2010; Stemann et al., 2013). Several authors have pointed out that the addition of acid to the reaction favors hydrolysis, decarboxylation, and dehydration of the raw wastes (Ameen et al., 2021; Aragón-Briceño et al., 2021; Sarrion et al., 2021). These reactions promote the release of a high content of organic matter in the process water, compared to that obtained without acid addition. However, the analysis of both process waters revealed minimal changes in the organic matter content (TCOD $28\text{--}34\text{ g L}^{-1}$, TOC $8\text{--}10\text{ g L}^{-1}$, and TVFA $\sim 2\text{ g L}^{-1}$), which could be attributed to a few subsequent

reactions that take place during HTC, such as aromatization, condensation and Maillard reactions. These reactions involve the formation of molecules of large molecular size from soluble organic compounds, which undergo transformations until they become solid particles that can be incorporated into the carbonaceous solid as secondary hydrochar (Ameen et al., 2021; Lucian et al., 2019). Consequently, soluble organic matter can be depleted from the liquid fraction and appears again as a precipitated solid phase (Ipiates et al., 2023b). Furthermore, the addition of acid to the reaction promotes the degree of carbonization of the hydrochar, which means higher carbon content and calorific value, as well as lower H/C and O/C atomic ratios (Aliyu et al., 2021).

Acid-assisted HTC significantly increased the migration and mineralization of nitrogen in the process water (Table 3) by improving the solubilization of nitrogen-containing organic compounds (NTK of $3.5\text{--}3.7\text{ g L}^{-1}$), almost double the value obtained from conventional HTC process water ($1.7\text{--}2.1\text{ g L}^{-1}$). TAN content in the acid-free process water reached values of $1.1\text{--}1.6\text{ g L}^{-1}$, which is 64–76% of TKN, the rest being organic nitrogen (Org-N). However, in the acid-treated HTC process water, almost all the Org-N was transformed to TAN ($> 95\%$). The $\text{NO}_3\text{-N}$ and $\text{NO}_2\text{-N}$ concentrations did not show relevant changes in process water. In acid-assisted HTC, phosphorus leaching as P-PO_4 was up to 8-fold higher (417 mg L^{-1}) compared to process water without acid (71 mg L^{-1}). In addition, acid-assisted HTC simultaneously promotes the migration of other elements such as Ca, Mg, K, Na, among others (Qaramaleki et al., 2020; Sarrion et al., 2022). Fig. 1 shows the distribution of N and P, two of the three essential nutrients for plant growth together with K. The amount of P leached from the SM to the non-acidic process water was very small ($3.5\text{--}5.5\text{ g P kg}^{-1}\text{ SM}$). Acid-assisted HTC promoted higher P leaching into the process water ($21.8\text{--}25.9\text{ g P kg}^{-1}\text{ SM}$). The amount of N in the SM was 24 g kg^{-1} (d. b.). Nitrogen migration was slightly higher in acidic process water $\sim 63\%$ ($\sim 14.5\text{ g N kg}^{-1}\text{ SM}$) than in acid-free process water 50–56% ($12.0\text{--}13.4\text{ g N kg}^{-1}\text{ SM}$). In acid-assisted HTC, total transformation of organic nitrogen to $\text{NH}_3\text{-N}$ was achieved (Fig. 1). $\text{NO}_3\text{-N}$ and $\text{NO}_2\text{-N}$ accounted less than 1% of the total nitrogen in the process water. In both cases, the increase in temperature slightly decreases the leaching of P and N in the process water. On the one hand, the increase in carbonization temperature favors the migration of other elements such as Ca, Al, Fe and Mg, which can react with PO_4^{3-} to form insoluble salts (Cui et al., 2020). On the other hand, the increase in N content at high carbonization temperatures can be attributed to the formation of pyrimidine, pyrrole and quaternary-N compounds, which are the basis of the secondary hydrochar structure (Krylova and Zaitchenko, 2018; Xiao et al., 2019).

The SM shows a high concentration of heavy metals (Table 1), which

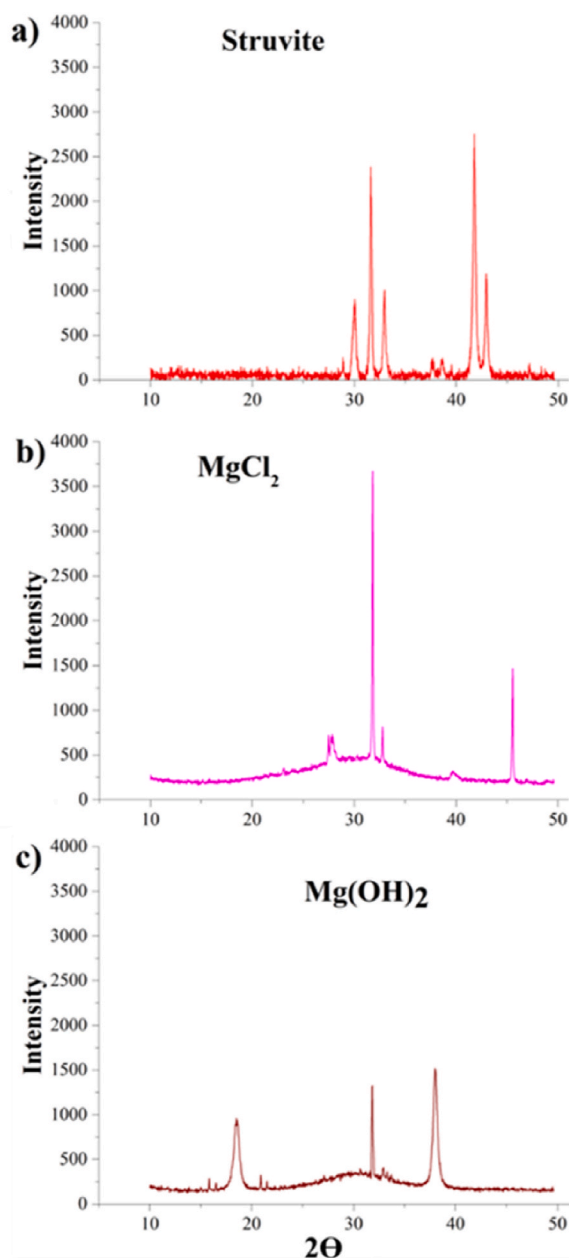


Fig. 2. X-ray diffractogram pattern of struvite (a) and precipitated solids from APW180 by addition of MgCl_2 (b) and Mg(OH)_2 (c).

came from feed, irrigation water, and agricultural chemicals. Their presence presents environmental risks, including soil and water pollution, toxicity to aquatic organisms and potential impacts on human health. Proper manure management is essential to mitigate these risks and preserve environmental and human health. Table S1 includes the limits of detection (LODs) and recoveries for heavy metal analysis. The heavy metals content into both conventional and acid-assisted process water was quantified (Table S2). Minor differences were observed between both process waters, indicating that the addition of HCl showed less influence on the migration of heavy metals in the process water than on mineral elements such as P, Ca, K, among others. Heavy metal content in process water is below inhibitory thresholds for anaerobic treatment: $\text{Cr} < 85 \text{ mg L}^{-1}$, $\text{Cd} < 34 \text{ mg L}^{-1}$, $\text{Ni} < 10 \text{ mg L}^{-1}$, and $\text{Pb} < 8 \text{ mg L}^{-1}$ (Chen et al., 2014).

Table 4

Mineral species (g kg^{-1}) and heavy metals (mg kg^{-1}) in precipitated solids^a with MgCl_2 and Mg(OH)_2 .

Mineral species (g kg^{-1})	Ca	Fe	K	Mg	N	Na	P
MgCl_2	6.6 (0.1)	2.0 (0.0)	4.5 (0.1)	133.0 (0.5)	78.0 (1.4)	1.1 (0.1)	167.3 (0.4)
Mg(OH)_2	19.0 (0.3)	1.3 (0.1)	3.7 (0.3)	167.4 (0.3)	38.4 (0.3)	0.7 (0.1)	41.8 (0.3)
Heavy metals (mg kg^{-1})	Cd	Co	Cr	Cu	Ni	Pb	Zn
MgCl_2	1.3 (0.0)	2.6 (0.1)	59.9 (0.3)	2.2 (0.1)	43.9 (0.2)	21.2 (0.2)	114.2 (1.3)
Mg(OH)_2	0.8 (0.0)	1.8 (0.1)	46.2 (0.1)	1.2 (0.1)	22.5 (0.5)	12.5 (0.1)	28.1 (0.1)

^a Average values of three determinations with standard deviations are shown in brackets.

3.2. Nutrient recovery

The acidic process water obtained at 180°C (APW180) was chosen for the nutrient recovery study because of its high concentration of $\text{PO}_4\text{-P}$ (417 mg L^{-1}), with respect to that obtained in the acid-free process water ($56\text{--}71 \text{ mg L}^{-1}$). Fig. 2 shows the XRD pattern of the precipitated solids using MgCl_2 and Mg(OH)_2 as reagents, while Table 4 shows the composition of these solids in mineral species and heavy metals. Struvite has been particularly appealing for recovery from process water streams (Becker et al., 2019; Shi et al., 2019). Analysis of the crystal structure of both solids revealed that the peaks obtained show little similarity to commercial struvite (Fig. 2a), with only the peak obtained at 30° dispersion angle (2θ) coinciding (RRUFF, 2023). The occurrence of these peaks can be attributed to the complexity of the process water and the presence of acid that leached a high amount of metallic elements in the process water. Certain metals such as Ca, Al, Fe, K can compete with Mg, interfering with the formation of struvite, giving rise to a mixture of various inorganic salts (Liu and Wang, 2019). However, due to the complexity of HTC process water, the formation of other inorganic salts such as apatite or hydroxyapatite (Wang et al., 2019, 2017) with high P content and other nutrients has also been reported (Ipiates et al., 2023a; Sarrion et al., 2023).

However, conventional HTC limits nutrient migration to process water, with acid-assisted HTC being a more advantageous alternative by maximizing nutrient migration to process water, while also improving hydrochar energy densification and combustion performance (Qaramaleki et al., 2020; Smith et al., 2020). Acid-assisted HTC can lixiviate 80% of divalent metals (Ca and Mg) and 50% of trivalent metals (Al and Fe) in the process water (Ipiates et al., 2023b). Nevertheless, despite not achieving a crystalline structure resembling struvite, the precipitated solid exhibited a high nutrients content, macronutrients, and low heavy metals content. Overall, the MgCl_2 proved to be a better reagent for the recovery of P and N, as it has a higher content of these nutrients, 167 g P kg^{-1} and 78 g N kg^{-1} , compared to Mg(OH)_2 (P: 41.8 g kg^{-1} and N: 38 g kg^{-1}). The presence of higher Ca (19 g kg^{-1}) and Mg (167 g kg^{-1}) content in the solid recovered with Mg(OH)_2 could indicate that the preferential formation of calcium phosphate salts as well as not solubilized Mg(OH)_2 . K exhibits a minor presence in the solid precipitate ($4\text{--}5 \text{ g kg}^{-1}$). After phosphorus precipitation, the TAN content in the process water was 0.94 g L^{-1} (an approximate recovery of 72%), while phosphorus was almost completely removed with a final concentration of 17.6 mg L^{-1} (an approximate removal of 95%). This process allowed the recovery of 20.7 g P kg^{-1} SM and 8.6 g N kg^{-1} SM. Finally, the NPK of the solid precipitates is $7.8/16.7/0.5$ for MgCl_2 and $3.8/4.2/0.4$ for Mg(OH)_2 . The heavy metal content in both solid precipitates is below the

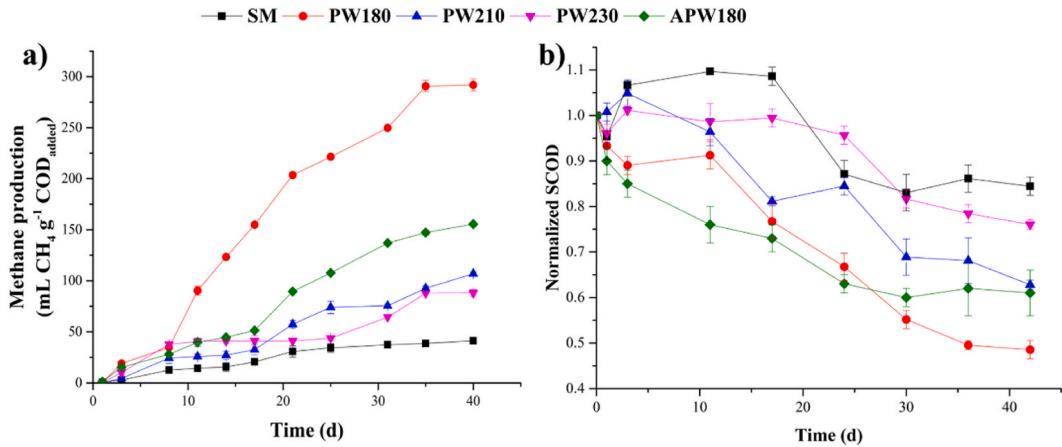


Fig. 3. Specific methane production of SM and process water (a) and normalized SCOD removal (b).

EU Regulation 2019/1009 (European Union, 2019) for the use of fertilizers and organic amendments in soils ($\text{Cd} < 2 \text{ mg kg}^{-1}$, $\text{Cr} < 200 \text{ mg kg}^{-1}$, $\text{Co} < 90 \text{ mg kg}^{-1}$, $\text{Pb} < 120 \text{ mg kg}^{-1}$, $\text{Cu} < 300 \text{ mg kg}^{-1}$ and $\text{Zn} < 800 \text{ mg kg}^{-1}$). However, there has been a recent development with the

implementation of Regulation CE 2021/2086 (European Commission, 2018), which actively supports the use of phosphate salts derived from recycled waste. Additionally, EU Regulation 2019/1009 has established criteria for fertilizers and soil amendments, facilitating the utilization

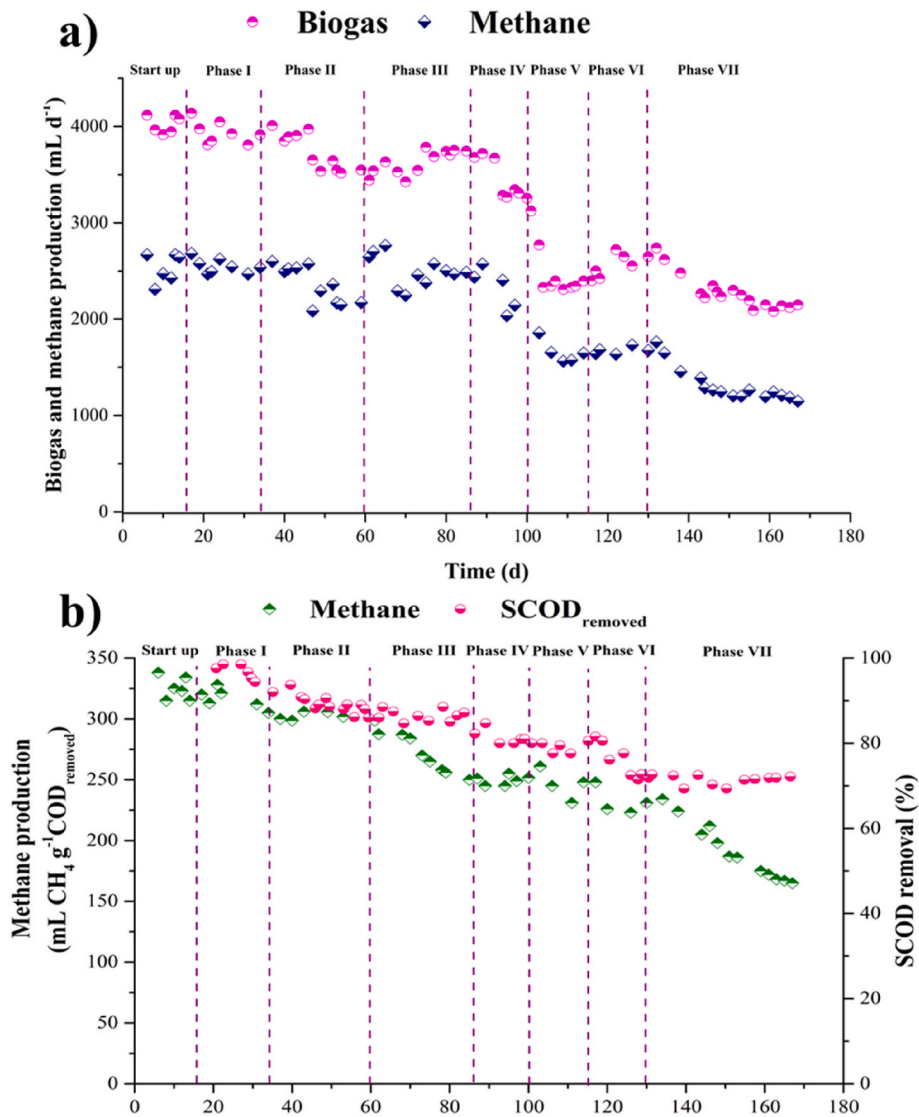


Fig. 4. Methane production and SCOD removal along anaerobic treatment of process water.

and commercialization of these recycled fertilizers in agricultural soils. Despite these regulatory advancements, a more in-depth evaluation is necessary to assess the potential of these phosphorus-rich solids. Comprehensive studies should explore their impact on plant germination, root growth, and stability in soils before considering their direct use.

3.3. Anaerobic digestion

3.3.1. Anaerobic digestion in batch mode

Fig. 3 shows the cumulative methane yield of SM and process water in batch mode (Fig. 3a) and normalized SCOD removal (Fig. 3b). SM was revealed to be an inappropriate substrate for AD with a very low methane production (~ 41 mL STP $\text{CH}_4 \text{ g}^{-1} \text{ COD}_{\text{added}}$) and low SCOD removal (14%), due to limited hydrolysis. PW180 yielded higher specific methane yield ~ 290 mL STP $\text{CH}_4 \text{ g}^{-1} \text{ COD}_{\text{added}}$ and a SCOD removal close to 55%. The increase in the HTC temperature negatively affected methane production which decreased up to 107 mL STP $\text{CH}_4 \text{ g}^{-1} \text{ COD}_{\text{added}}$ and SCOD removal close to 35% for PW230. The acid-assisted HTC also affected AD negatively but less than temperature. In this way the APW180 yielded 164 mL STP $\text{CH}_4 \text{ g}^{-1} \text{ COD}_{\text{added}}$ and ~ 17 percentage points less SCOD removal than PW180. The low methane production and organic matter removal in the case of PW210, PW230 and APW180 could be explained by the formation of more complex organic compounds into the process water (see Table S3 and S4). Furthermore, acid-assisted HTC could be inhibitory to methanogenic microorganisms due to the presence of chloride (Ni et al., 2022). To improve the understanding of anaerobic biodegradability, a more detailed analysis of the organic composition of the process water was performed. Fig. S2 shows the organic species detected in PW180 at different reaction times (5, 15, 30 and 60 min), while Fig. S3 shows the analysis of the process water obtained from HTC at 180 °C in the presence and absence of acid after 60 min of reaction. In addition, Tables S2 and S3 show the composition and peak areas of those organic compounds. At long reaction times, in PW180, the diversity and concentration of organic species increased, especially O- and N-containing compounds (such as pyrazines, pyrimidines, pyridine and indole), aromatics (phenol, furfural) and long-chain alkyl species (Fig. S2 and Table S3).

The increase in temperature showed an impact comparable to that of residence time, resulting in a reduction of aliphatic compounds and a gradual increase in the presence of more complex compounds (aromatics and heteroatoms) (see Table S2). However, in APW180 the most significant change was observed in the furfural yield, up to 6 times more peak area compared to PW180, suggesting that the addition of acid enhanced the hydrolysis and dehydration of sugars (Table S3). In addition, there was a remarkable decrease of compounds such as aromatics, O- and N-compounds in APW180, which could probably be attributed to their degradation or involvement in secondary hydrochar formation. According to Lucian et al. (2019), the high aromatic content and the presence of O- and N-heteroatoms act as a block to secondary hydrochar formation. Similar trend was found by Ipiales et al. (2023a) with a reduction of O- and N-heteroatoms during co-HTC of lignocellulosic waste and SM yielding a moderate increase in hydrochar mass yield probably due to secondary hydrochar formation. Several pharmaceutical compounds such as penicillamine, prednisolone acetate, aldosterone among others detected in SM were degraded during conventional HTC except for penicillamine (see Table S3). Although, temperature increase or addition of acid totally degraded penicillamine (see Table S3 and S4).

The highest energy recovery was achieved from the process water at the lowest carbonization temperatures (180 °C), reaching 3.8 MJ kg^{-1} SM ($\sim 24.4\%$) from conventional HTC and 2.5 MJ kg^{-1} SM ($\sim 15.8\%$) from acid-assisted HTC of the energy contained in the SM. With increasing temperature, energy recovery decreased due to lower methane production, in the range 0.9–1.3 MJ kg^{-1} SM. It is noteworthy that direct treatment of SM, without any pretreatment, only allowed a

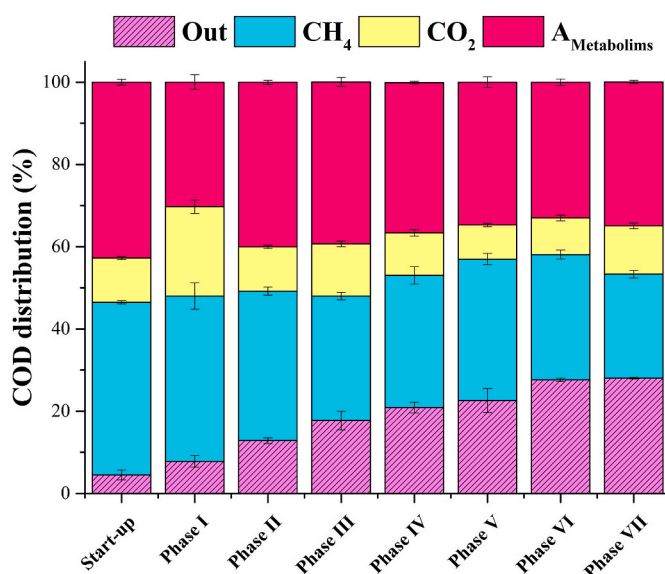


Fig. 5. COD distribution along the anaerobic treatment stages.

recovery of 2.2 MJ kg^{-1} ($\sim 13.9\%$), indicating that direct anaerobic treatment of SM is not an attractive alternative for the management of this waste. Several authors highlight that hydrochar can retain up to 75% of the energy contained in the raw biomass (Ipiales et al., 2021; Marin-Batista et al., 2019), therefore the carbonization of biomass waste, such as swine manure, in hydrochar together with the treatment of process water by anaerobic digestion represents an efficient alternative for the management of this waste.

3.3.2. Anaerobic digestion of process water in continuous mode

Fig. 4 displays the biogas and methane production (Fig. 4a), as well as the methane production yield per gram of SCOD removed and the SCOD removal rate (Fig. 4b). During the reactor startup with 100% COD from glucose (G), the highest methane production rate of 330 mL STP $\text{CH}_4 \text{ g}^{-1} \text{ COD}_{\text{removed}}$ (~ 2600 mL $\text{CH}_4 \text{ L}^{-1} \text{ d}^{-1}$) was achieved, close to the theoretical value. This outcome was expected since glucose is an easily biodegradable organic compound with a COD removal around 97%. However, methane production rate, daily biogas production and SCOD removal gradually decreased as the process water fed increased. In phase I (90/10 G/PW), methane production dropped below the theoretical value to 310 mL STP $\text{CH}_4 \text{ g}^{-1} \text{ COD}_{\text{removed}}$ (2100 mL $\text{CH}_4 \text{ L}^{-1} \text{ d}^{-1}$), with a SCOD removal rate around 93%. This progressive reduction continued until phases V and VI (50/50 and 40/60 G/PW, respectively), where stable methane production (230 mL STP $\text{CH}_4 \text{ g}^{-1} \text{ COD}_{\text{removed}}$) and SCOD removal ($\sim 80\%$) were observed despite the increase of process water in the feed. Finally, with a 25/75 G/PW ratio in the feed, a significant decrease in methane production (~ 180 mL STP $\text{CH}_4 \text{ g}^{-1} \text{ COD}_{\text{removed}}$) and SCOD removal (70%) was observed.

Although the pH 6.5–7.5 and alkalinity >2000 mg $\text{CaCO}_3 \text{ L}^{-1}$ of the system were maintained throughout the assay, a steady decline in methane production was observed in phase VII, possibly due to system instability. This decline in methane production rate and organic matter removal, especially pronounced in phase VII, could be attributed to the characteristics of the process water source. The raw SM showed a C/N ratio close to 0.7. After conventional HTC at 180 °C, the C/N ratio increased to 3.2, but was still below the ideal C/N ratio for anaerobic treatment, which is usually between 20 and 30. Mixing SM with glucose (a carbon-rich substrate) significantly improved the C/N ratio. In phase I, the C/N ratio was 13.5, but decreased to 3.7 in phase VII, approaching the value of PW180. This suggests that process water from HTC of SM should be supplemented with another waste effluent for anaerobic co-digestion or, alternatively, perform hydrothermal co-carbonization

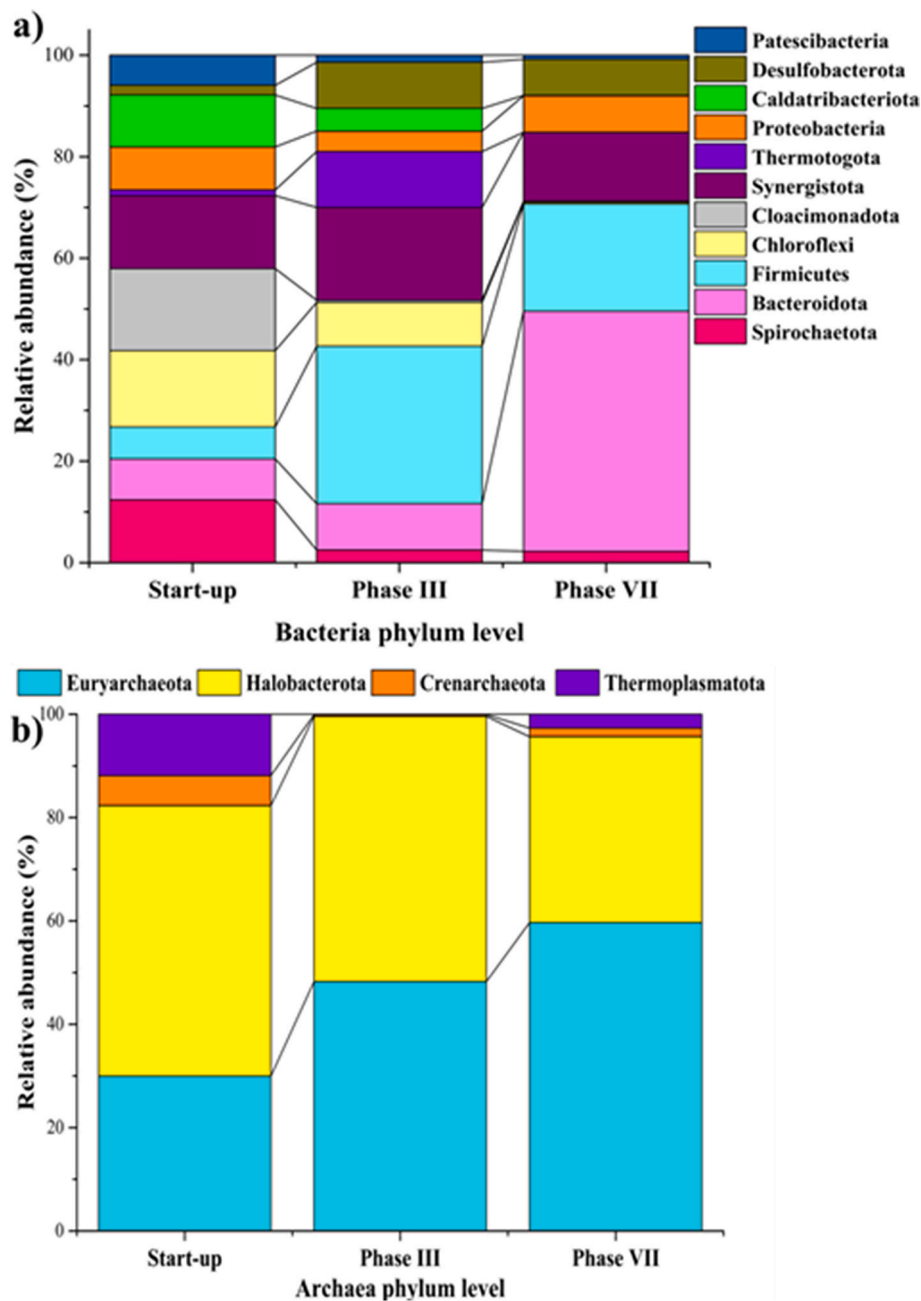


Fig. 6. Microbial community of bacteria (a) and archaea (b) at phylum level.

with another carbon-rich residue, such as lignocellulosic biomass. Actually, the process water from the co-HTC of 25% SM and 75% lignocellulosic biomass, had a C/N ratio of approximately 45 (Ipiales et al., 2023a).

UASB (Liu et al., 2021) and three-stage and semi-industrial anaerobic system (CSTR and EGSB) (Weide et al., 2019) reactors configurations in HTC process water treatment present similar performances to those obtained, with methane production yield of 250–300 mL CH₄ g⁻¹ COD_{removed} and SCOD removal of 70–80%, with a lower OLR (1.9–3.3 g COD L⁻¹ d⁻¹) than those used in this study. Wirth and Mumme (2013) observed that nutrient deficiency in the process water from HTC of corn silage could be one of the limiting factors in successful anaerobic treatment of process water. Some authors emphasized that one limitation of the anaerobic treatment of process water was the medium acidification (Ahmed et al., 2021; Wirth et al., 2015), which suggests that the initial stages of hydrolysis, acidogenesis, and acetogenesis are

unaffected, but the methanogenic phase is impacted by the accumulation of VFA. Franke-Whittle et al. (2014) observed that methanogenic archaea were the most sensitive anaerobic microorganisms, while other microbial consortia are more resistant. Ahmed et al. (2021) also suggests that the addition of hydrochar into the anaerobic treatment of process water of sewage sludge could help alleviate certain limitations, including medium acidification.

Fig. 5 shows the COD balance throughout the anaerobic treatment of the process water. The COD balance was calculated using the results of the last 4 days of each stage after reaching steady state. During start-up, COD consumption is very efficient, with a minimal fraction remaining in the effluent (<5% COD). Approximately 53% of the SCOD was directed towards biogas production, 42% to CH₄ (3.4 g COD d⁻¹) and 11% to CO₂ (0.9 g COD d⁻¹), while a significant portion of the organic matter, fed in form of COD, was used for the maintenance and metabolism of the anaerobic consortium ~ 43% (3.4 g COD d⁻¹). The introduction of

process water into the system caused a decrease in the consumption of organic matter in form of COD, both for CH₄ production and maintenance of microorganisms. COD in the effluent gradually increased from 8% (0.6 g COD d⁻¹) in phase I to 28% (2.2 g COD d⁻¹) in phase VII. In addition, less COD was used for CH₄ production, which decreased from 40% (3.2 g COD d⁻¹) in phase I to 25% (2 g COD d⁻¹) in phase VII. COD removal as CO₂ showed minimal variations throughout the reaction 9–12% (0.7–0.9 g COD d⁻¹). On the other hand, microorganism maintenance decreased from 41% (3.3 g COD d⁻¹) in phase I to 35% (2.8 g COD d⁻¹) at the end of the experiment.

3.4. Microbial community

The complexity of process water requires a deep understanding of the evolution and adaptation of microbial communities during the anaerobic treatment. Typically, anaerobic inocula are composed of a wide diversity of microorganisms: fermenting, acidogens, acetogens bacteria and methanogens archaea (Li et al., 2021). The initial inoculum is characterized by a highly diverse bacterial community dominated by Spirochaetota, Chloroflexi, Cloacimonadota and Synergistota at the bacterial level (Fig. 6a) and by Euryarchaeota and Halobacterota in the archaea level (Fig. 6b). The percentage of archaea in the initial inoculum was 17%, indicating that the initial inoculum is rich in hydrolytic, acidogenic and acetogenic bacteria, with a lower percentage of microorganisms responsible for methane production. As expected, feeding the reactor with process water significantly influenced the evolution of the inoculum. Thus, the genus Spirochaeta decreased to represent <3% of the total anaerobic bacteria. Bacteroidota and Firmicutes phyla, known to promote the hydrolysis of complex organic compounds such as proteins, amino acids, cellulose and aromatic compounds (St-Pierre and Wright, 2014), became the dominant phyla. In the case of archaea, Euryarchaeota and Halobacterota maintained their presence in the early stages of the anaerobic process. In stage III, archaea played a more important role, growing and representing up to 35% of the total diversity of the microbial community, in accordance with the methane production (300 mL g⁻¹ COD_{removed}) and SCOD removal (85%) obtained. However, in stage VII, their presence decreased, representing only 10% associated with a lower methane production. Similarly, phylum-level analysis of the bacteria showed that the microorganisms that proliferated the most were those capable of degrading organic nitrogen compounds, which is consistent with the C/N ratio of the process water. Liu et al. (2021) observed a high increase of Firmicutes and Acidobacteria, responsible for degrading nitrogenous compounds into NH₃-N and converting organic compounds into VFA. This suggests that the process water does not significantly affect the microorganisms responsible for carrying out these transformations but seems to affect the methanogenic archaea responsible for converting these volatile organic acids into methane.

4. Conclusions

The study addresses two strategies for the valorization of HTC process water from swine manure. Conventional HTC process water did not contain an interesting concentration of nutrients (P and N) to consider their reclamation, being energy recovery a more suitable alternative. Anaerobic digestion of those effluents in batch trials indicated that increasing the HTC temperature showed a negative impact on methane production and organic matter removal, providing the process water obtained at 180 °C the best results. The continuous experiment conducted in an UASB reactor showed high COD removal efficiency, close to 70%, and a methane production around 180 mL STP g⁻¹ COD_{removed}. The decrease in methane production efficiency was due to a decrease in the C/N ratio as the proportion of process water in the feed increased. Therefore, to enhance the performance of anaerobic treatment, it is advisable to blend it with another liquid waste rich in carbon or, alternatively, undergo a pre-mixing before HTC (hydrothermal co-

carbonization) to improve the C/N ratio of the liquid effluent. The study of the microbial population revealed a loss of methanogenic archaea and an increase in bacteria capable of degrading nitrogen-containing organic compounds and hydrolytic-acidogenic bacteria along the process. Nutrient recovery was the most promising alternative to valorize the acid-assisted HTC process water, due to the high phosphorus content in the liquid fraction (84% of the P in the SM). Phosphorus precipitation with magnesium salts did not provide struvite formation due to the high complexity of the process water. However, precipitated solids showed a high P and N content especially using MgCl₂ as Mg source, together with a heavy metal content below the limits established by EU Regulation 2019/1009.

CRediT authorship contribution statement

R.P. Ipiales: Writing – original draft, Investigation, Formal analysis, Conceptualization. **G. Lelli:** Writing – original draft, Investigation, Formal analysis. **E. Diaz:** Writing – review & editing, Supervision, Resources, Funding acquisition. **E. Diaz-Portuondo:** Supervision, Resources, Funding acquisition, Formal analysis, Conceptualization. **A.F. Mohedano:** Writing – review & editing, Supervision, Resources, Project administration, Methodology, Funding acquisition, Conceptualization. **M.A. de la Rubia:** Writing – review & editing, Supervision, Resources, Project administration, Methodology, Funding acquisition, Conceptualization.

Declaration of competing interest

The authors declare that they have no known competing financial interests or personal relationships that could have appeared to influence the work reported in this paper.

Data availability

Data will be made available on request.

Acknowledgements

Authors greatly appreciate funding from Spanish MCIN/AEI/10.13039/501100011033 and European Union "NextGenerationEU/PRTR" (TED2021-130287B-I00, PDC 2021-120755-I00, and PID 2022-138632OB-I00) and Grupo Kerbest Company. R.P. Ipiales acknowledges the financial support from the Community of Madrid (IND2019/AMB-17092) and Arquimea Agrotech Company.

Appendix A. Supplementary data

Supplementary data to this article can be found online at <https://doi.org/10.1016/j.envres.2024.118098>.

References

- Ahmed, M., Sartori, F., Merzari, F., Fiori, L., Elagroudy, S., Negm, M.S., Andreottola, G., 2021. Anaerobic degradation of digestate based hydrothermal carbonization products in a continuous hybrid fixed bed anaerobic filter. *Bioresour. Technol.* 330, 124971 <https://doi.org/10.1016/j.biortech.2021.124971>.
- Aliyu, M., Iwabuchi, K., Itoh, T., 2021. Upgrading the fuel properties of hydrochar by co-hydrothermal carbonisation of dairy manure and Japanese larch (*Larix kaempferi*): product characterisation, thermal behaviour, kinetics and thermodynamic properties. *Biomass Convers. Biorefinery*. <https://doi.org/10.1007/s13399-021-02045-0>.
- Ameen, M., Zamri, N.M., May, S.T., Azizan, M.T., Aqsha, A., 2021. Effect of acid catalysts on hydrothermal carbonization of Malaysian oil palm residues (leaves, fronds, and shells) for hydrochar production. *Biomass Conv. Biorefin.* 1–12 <https://doi.org/10.1007/s13399-020-01201-2>.
- Angelidaki, I., Sanders, W., 2004. Assessment of the anaerobic biodegradability of macropollutants. *Rev. Environ. Sci. Biotechnol.* 3, 117–129. <https://doi.org/10.1007/s11157-004-2502-3>.
- APHA, 2005. *Standard Methods for the Examination of Water and Wastewater*, twenty-first ed. American Public Health Association, Washington, DC, USA.

- Aragón-Briceno, C.I., Pozarlik, A.K., Bramer, E.A., Niedzwiecki, L., Pawlak-Kruczek, H., Brem, G., 2021. Hydrothermal carbonization of wet biomass from nitrogen and phosphorus approach: a review. *Renew. Energy* 171, 401–415. <https://doi.org/10.1016/j.renene.2021.02.109>.
- Becker, G.C., Wüst, D., Köhler, H., Lautenbach, A., Kruse, A., 2019. Novel approach of phosphate-reclamation as struvite from sewage sludge by utilising hydrothermal carbonization. *J. Environ. Manage.* 238, 119–125. <https://doi.org/10.1016/j.jenvman.2019.02.121>.
- Bianchini, A., Bonfiglioli, L., Pellegrini, M., Saccani, C., 2016. Sewage sludge management in Europe: a critical analysis of data quality. *Environ. Waste Manag.* 18, 226–238. <https://doi.org/10.1504/IJEW.2016.10001645>.
- Bloem, E., Albihn, A., Elving, J., Hermann, L., Lehmann, L., Sarvi, M., Schaaf, T., Schick, J., Turtola, E., Ylivainio, K., 2017. Contamination of organic nutrient sources with potentially toxic elements, antibiotics and pathogen microorganisms in relation to P fertilizer potential and treatment options for the production of sustainable fertilizers: a review, 607 *Sci. Total Environ* 608, 225–242. <https://doi.org/10.1016/j.scitotenv.2017.06.274>.
- Buckel, W., 2021. Energy conservation in fermentations of anaerobic bacteria. *Front. Microbiol.* 12, 1–16. <https://doi.org/10.3389/fmicb.2021.703525>.
- Chen, J.L., Ortiz, R., Steele, T.W.J., Stuckey, D.C., 2014. Toxicants inhibiting anaerobic digestion: a review. *Biotechnol. Adv.* 32, 1523–1534. <https://doi.org/10.1016/J.BIOTECHADV.2014.10.005>.
- Cui, X., Lu, M., Khan, M.B., Lai, C., Yang, X., He, Z., Chen, G., Yan, B., 2020. Hydrothermal carbonization of different wetland biomass wastes: phosphorus reclamation and hydrochar production. *Waste Manag.* 102, 106–113. <https://doi.org/10.1016/j.wasman.2019.10.034>.
- De la Rubia, M.A., Villamil, J.A., Rodriguez, J.J., Borja, R., Mohedano, A.F., 2018. Mesophilic anaerobic co-digestion of the organic fraction of municipal solid waste with the liquid fraction from hydrothermal carbonization of sewage sludge. *Waste Manag.* 76, 315–322. <https://doi.org/10.1016/j.wasman.2018.02.046>.
- European Commission, 2018. COMMISSION DELEGATED REGULATION (EU) 2021/2086 of 5 July 2021 Amending Annexes II and IV to Regulation (EU) 2019/1009 of the European Parliament and of the Council for the Purpose of Adding Precipitated Phosphate Salts and Derivates as a Component Materia. <https://doi.org/10.2760/186684>.
- European Union, 2019. 1009 of the European Parliament and of the Council of 5 June 2019 Laying Down Rules on the Making Available on the Market of EU Fertilising Products and Amending Regulations (EC) No 1069/2009 and (EC) No 1107/2009 and Repealing R. Regulation, E. U. (2019).
- EUROSTAT, 2020. Agricultural Census 2020.
- Franke-Whittle, I.H., Walter, A., Ebner, C., Insam, H., 2014. Investigation into the effect of high concentrations of volatile fatty acids in anaerobic digestion on methanogenic communities. *Waste Manag.* 34, 2080–2089. <https://doi.org/10.1016/j.wasman.2014.07.020>.
- Funke, A., Ziegler, F., 2010. Hydrothermal carbonization of biomass: a summary and discussion of chemical mechanisms for process engineering. *Biofuels, Bioprod. Biorefining* 4, 160–177. <https://doi.org/10.1002/bbb.198>.
- He, X., Wang, Y., Zhang, Y., Wang, C., Yu, J., Ohtake, H., Zhang, T., 2023. The potential for livestock manure valorization and phosphorus recovery by hydrothermal technology - a critical review. *Mater. Sci. Energy Technol.* 6, 94–104. <https://doi.org/10.1016/j.mset.2022.11.008>.
- Heidari, M., Salaudeen, S., Norouzi, O., Acharya, B., Dutta, A., 2020. Numerical comparison of a combined hydrothermal carbonization and anaerobic digestion system with direct combustion of biomass for power production. *Processes* 8 (43), 1–13. <https://doi.org/10.3390/pr8010043>.
- Ipiates, R.P., de la Rubia, M.A., Diaz, E., Mohedano, A.F., Rodriguez, J.J., 2021. Integration of hydrothermal carbonization and anaerobic digestion for energy recovery of biomass waste: an overview. *Energy Fuel* 35, 17032–17050. <https://doi.org/10.1021/acs.energyfuels.1c01681>.
- Ipiates, R.P., Mohedano, A.F., Diaz-Portuondo, E., Diaz, E., De la Rubia, M.A., 2023a. Co-hydrothermal carbonization of swine manure and lignocellulosic waste : a new strategy for the integral valorization of biomass wastes. *Waste Manag.* 169, 267–275. <https://doi.org/10.1016/j.wasman.2023.07.018>.
- Ipiates, R.P., Sarrion, A., Diaz, E., Diaz-Portuondo, E., Mohedano, A.F., de la Rubia, A., 2023b. Strategies to improve swine manure hydrochar: HCl-assisted hydrothermal carbonization versus hydrochar washing. *Biomass Convers. Biorefinery* 1–12. <https://doi.org/10.1007/s13399-023-04027-w>.
- Khosravi, A., Zheng, H., Liu, Q., Hashemi, M., Tang, Y., Xing, B., 2022. Production and characterization of hydrochars and their application in soil improvement and environmental remediation. *Chem. Eng. J.* 430, 133142. <https://doi.org/10.1016/J.CEJ.2021.133142>.
- Königer, J., Lugato, E., Panagos, P., Kochupillai, M., Orgiazzi, A., Briones, M.J.I., 2021. Manure management and soil biodiversity: towards more sustainable food systems in the EU. *Agric. Syst.* 194. <https://doi.org/10.1016/j.agry.2021.103251>.
- Krylova, A.Y., Zaitchenko, V.M., 2018. Hydrothermal carbonization of biomass : a review. *Solid Fuel Chem.* 52, 91–103. <https://doi.org/10.3103/S0361521918020076>.
- Li, Y., Xu, H., Yi, X., Zhao, Y., Jin, F., Chen, L., Hua, D., 2021. Study of two-phase anaerobic digestion of corn stover: focusing on the conversion of volatile fatty acids and microbial characteristics in UASB reactor. *Ind. Crops Prod.* 160, 113097. <https://doi.org/10.1016/j.indcrop.2020.113097>.
- Liu, S., Wang, Y., Guo, J., Wang, W., Dong, R., 2021. Start-up and performance evaluation of upflow anaerobic sludge blanket reactor treating supernatant of hydrothermally treated municipal sludge: effect of initial organic loading rate. *Biochem. Eng. J.* 166, 107843. <https://doi.org/10.1016/j.bej.2020.107843>.
- Liu, X., Wang, J., 2019. Impact of calcium on struvite crystallization in the wastewater and its competition with magnesium. *Chem. Eng. J.* 378, 122121. <https://doi.org/10.1016/j.cej.2019.122121>.
- Lucian, M., Volpe, M., Fiori, L., 2019. Hydrothermal carbonization kinetics of lignocellulosic agro-wastes: experimental data and modeling. *Energies* 12, 1–20. <https://doi.org/10.3390/en12030516>.
- Marin-Batista, J.D., Villamil, J.A., Rodriguez, J.J., Mohedano, A.F., De la Rubia, M.A., 2019. Valorization of microalgal biomass by hydrothermal carbonization and anaerobic digestion. *Bioresour. Technol.* 274, 395–402. <https://doi.org/10.1016/j.biortech.2018.11.103>.
- Ni, J., Ji, J., Kubota, K., Li, Y.-Y., 2022. Sodium hypochlorite induced inhibition in anaerobic digestion and possible approach to maintain methane fermentation performance. *Bioresour. Technol.* 352, 127096. <https://doi.org/10.1016/j.biortech.2022.127096>.
- Numviyimana, C., Warchol, J., Khalaf, N., Leahy, J.J., Chojnacka, K., 2022. Phosphorus recovery as struvite from hydrothermal carbonization liquor of chemically produced dairy sludge by extraction and precipitation. *J. Environ. Chem. Eng.* 10, 106947. <https://doi.org/10.1016/j.jece.2021.106947>.
- Oelgeschläger, E., Rother, M., 2008. Carbon monoxide-dependent energy metabolism in anaerobic bacteria and archaea. *Arch. Microbiol.* 190, 257–269. <https://doi.org/10.1007/s00203-008-0382-6>.
- Qaramaleki, S.V., Villamil, J.A., Mohedano, A.F., Coronella, C.J., 2020. Factors affecting solubilization of phosphorus and nitrogen through hydrothermal carbonization of animal manure. *ACS Sustain. Chem. Eng.* 8, 12462–12470. <https://doi.org/10.1021/acscuschemeng.0c03268>.
- Raposo, F., de la Rubia, M.A., Borja, R., Alaiz, M., 2008. Assessment of a modified and optimised method for determining chemical oxygen demand of solid substrates and solutions with high suspended solid content. *Talanta* 76, 448–453. <https://doi.org/10.1016/j.talanta.2008.03.030>.
- RRUFF, 2023. Database of Raman spectroscopy, X-Ray diffraction and chemistry of minerals [WWW Document].
- Sarrion, A., de la Rubia, A., Coronella, C., Mohedano, A.F., Diaz, E., 2022. Acid-mediated hydrothermal treatment of sewage sludge for nutrient recovery. *Sci. Total Environ.* 156494. <https://doi.org/10.1016/j.scitotenv.2022.156494>.
- Sarrion, A., Diaz, E., Angeles de la Rubia, M., Mohedano, A.F., 2021. Fate of nutrients during hydrothermal treatment of food waste. *Bioresour. Technol.* 125954. <https://doi.org/10.1016/j.biortech.2021.125954>.
- Sarrion, A., Ipiates, R.P., de la Rubia, M.A., Mohedano, A.F., Diaz, E., 2023. Chicken meat and bone meal valorization by hydrothermal treatment and anaerobic digestion: biofuel production and nutrient recovery. *Renew. Energy* 204, 652–660. <https://doi.org/10.1016/j.renene.2023.01.005>.
- Sharma, R., Jasrotia, K., Singh, N., Ghosh, P., Srivastava, S., Sharma, N.R., Singh, J., Kanwar, R., Kumar, A., 2020. A comprehensive review on hydrothermal carbonization of biomass and its applications. *Chem. Africa* 3, 1–19. <https://doi.org/10.1016/s24250-019-00098-3>.
- Shi, Y., Luo, G., Rao, Y., Chen, H., Zhang, S., 2019. Hydrothermal conversion of dewatered sewage sludge: focusing on the transformation mechanism and recovery of phosphorus. *Chemosphere* 228, 619–628. <https://doi.org/10.1016/j.chemosphere.2019.04.109>.
- Smith, A.M., Ekpo, U., Ross, A.B., 2020. The influence of pH on the combustion properties of bio-coal following hydrothermal treatment of swine manure. *Energies* 13, 1–20. <https://doi.org/10.3390/en13020331>.
- St-Pierre, B., Wright, A.D.G., 2014. Comparative metagenomic analysis of bacterial populations in three full-scale mesophilic anaerobic manure digesters. *Appl. Microbiol. Biotechnol.* 98, 2709–2717. <https://doi.org/10.1007/s00253-013-5220-3>.
- Stemann, J., Putschew, A., Ziegler, F., 2013. Hydrothermal carbonization: process water characterization and effects of water recirculation. *Bioresour. Technol.* 143, 139–146. <https://doi.org/10.1016/j.biortech.2013.05.098>.
- Villamil, J.A., Mohedano, A.F., Rodriguez, J.J., De la Rubia, M.A., 2018. Valorisation of the liquid fraction from hydrothermal carbonisation of sewage sludge by anaerobic digestion. *J. Chem. Technol. Biotechnol.* 93, 450–456. <https://doi.org/10.1002/jctb.5375>.
- Wang, L., Chang, Y., Liu, Q., 2019. Fate and distribution of nutrients and heavy metals during hydrothermal carbonization of sewage sludge with implication to land application. *J. Clean. Prod.* 225, 972–983. <https://doi.org/10.1016/j.jclepro.2019.03.347>.
- Wang, Tao, Zhai, Y., Zhu, Y., Peng, C., Wang, Tengfei, Xu, B., Li, C., Zeng, G., 2017. Feedwater pH affects phosphorus transformation during hydrothermal carbonization of sewage sludge. *Bioresour. Technol.* 245, 182–187. <https://doi.org/10.1016/j.biortech.2017.08.114>.
- Weide, T., Brüggling, E., Wetter, C., 2019. Anaerobic and aerobic degradation of wastewater from hydrothermal carbonization (HTC) in a continuous, three-stage and semi-industrial system. *J. Environ. Chem. Eng.* 7, 102912. <https://doi.org/10.1016/j.jece.2019.102912>.
- Weideler, A., Krampe, J., Steinmetz, H., 2008. Phosphorrückgewinnung aus kommunalem Klärschlamm als Magnesium-Ammonium-Phosphat (MAP). *Wasser Abfall* 23–26.
- Wirth, B., Mumme, J., 2013. Anaerobic digestion of waste water from hydrothermal carbonization of corn silage. *Appl. Bioenergy* 1–10. <https://doi.org/10.2478/apbi-2013-0001>.
- Wirth, B., Reza, T., Mumme, J., 2015. Influence of digestion temperature and organic loading rate on the continuous anaerobic treatment of process liquor from

- hydrothermal carbonization of sewage sludge. *Bioresour. Technol.* 198, 215–222. <https://doi.org/10.1016/j.biortech.2015.09.022>.
- Xiao, H., Zhai, Y., Xie, J., Wang, T., Wang, B., Li, S., Li, C., 2019. Speciation and transformation of nitrogen for spirulina hydrothermal carbonization. *Bioresour. Technol.* 286, 121385 <https://doi.org/10.1016/j.biortech.2019.121385>.
- Zahedi, Gros, M., Petrović, M., Balcazar, J.L., Pijuan, M., 2022. Anaerobic treatment of swine manure under mesophilic and thermophilic temperatures: fate of veterinary drugs and resistance genes. *Sci. Total Environ.* 818 <https://doi.org/10.1016/j.scitotenv.2021.151697>.